# Effects of Substrate Constraint on Crack Pattern Formation in Thin Films of Colloidal Polystyrene Particles

M. I. Smith and J. S. Sharp*

School of Physics and Astronomy and Nottingham Nanotechnology and Nanoscience Centre, University of Nottingham, University Park, Nottingham, NG7 2RD, U.K.

ABSTRACT: Crack formation and the evolution of stress in drying films of colloidal particles were studied using optical microscopy and a modified cantilever deflection technique, respectively. Drying experiments were performed using polystyrene particles with diameters of 47 ± 10 nm, 100 ± 16 nm, and 274 ± 44 nm that were suspended in water. As the films dried, cracks with a well-defined spacing were observed to form. The crack spacing was found to be independent of the particle size used, but to increase with the film thickness. The characteristic crack spacing was found to vary between 20 and 300 μm for films with thickness values in the range $3-70$ μm. Cantilever deflection measurements revealed that the stresses that develop in the film increase with decreasing film thickness (increasing surface-to-volume ratio). The latter observation was interpreted in terms of the effects of a substrate constraint which causes the build up of stresses in the films. This interpretation was confirmed by crack formation experiments that were performed on liquid mercury surfaces in which removal of the substrate constraint prevented crack formation. Experiments were also performed on compliant elastomer surfaces in which the level of constraint was varied by changing the substrate modulus. The cracking length scale was found to increase with decreasing substrate modulus. A simple theory was also developed to describe the substrate modulus dependence of the cracking length scale. These combined experiments and theory provide convincing evidence that substrate constraints are an important factor in driving crack formation in thin colloidal films.
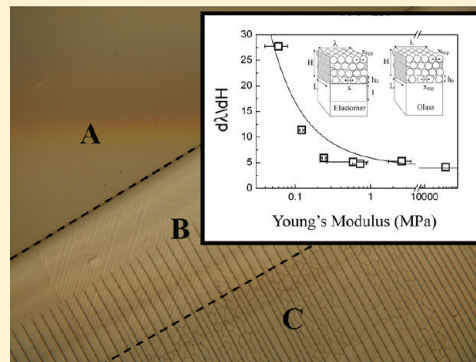
INTRODUCTION

Crack formation during the drying of thin films of colloidal particles is a common technological problem found in the production of ceramic coatings, paints, and glazes.[1] These systems are usually formed from a reservoir of colloidal suspended particles that are spread on a substrate. The suspension then begins to dry and as the suspending liquid (usually water) evaporates, particles are pulled into contact by liquid bridges that form between the particles as the films dry out. Depending upon their rigidity, the particles either deform under the influence of these capillary forces or tightly pack into a thin film.[2]

The cracks that are commonly observed to form during the drying of close packed particle films are usually undesirable from a commercial point of view, and these effects have largely been overcome by the inclusion of binding agents or plasticizers. However, the process of crack formation continues to retain a great deal of scientific interest due to the complex nature of the cracking mechanism. When cracks form, they are usually observed to grow in wet regions of the film (region B, Figure 1) where the particles are close packed but the void space between them is still filled with liquid. The initial cracks that form tend to be oriented in a direction perpendicular to the drying surface and the crack tips remain at an approximately constant distance from the retreating reservoir and the drying front. Capillary forces at the upper surface place the wet portion of the film (region B,

Figure 1) under a corresponding capillary stress $\sim \gamma/R$ (where γ and R are the surface tension of the liquid and the radius of the suspended particles, respectively). If this stress exceeds the yield stress of the packed particle films, the strain energy stored in the film can be released by creating new interfaces and redistributing the fluid in the films; a crack is formed.[3] This energy-based approach is rather simplistic, but it captures the essential physics of the cracking process. Details of the precise mechanism of crack formation have been debated for some time with a number of different models being proposed.[4−8]

Given the importance of capillary forces during drying, the particle size might be expected to play a significant role in determining the crack spacing. Chiu et al.[9] found a strong particle size dependence of the critical cracking thickness (a film thickness below which films do not crack) in films of alumina particles. A recent study by Cao et al.[10] also found that the crack spacing in a vertical drying film shows a particle size dependence. However, the drying geometries and methods used in these previous studies were different from those described in the study presented below, where no particle size dependence is observed.
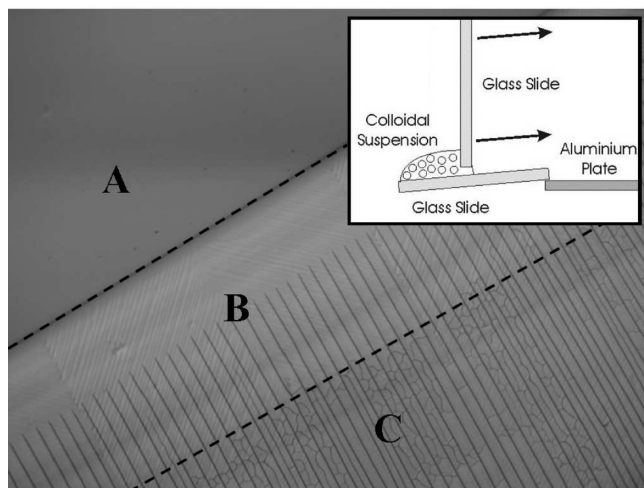
Figure 1. Optical micrograph of a planar drying front in a colloidal film of 47 nm polystyrene particles. Three distinct regions can be observed: region A corresponds to the dilute colloidal suspension, region B consists of closely packed colloidal particles with water filling the void space, and region C consists of a 'dry' closely packed film. The inset in this figure shows how the films are cast. Droplets of the colloidal suspension are deposited along the bottom edge of a glass slide that has its upper edge supported on a ~ 1 mm thick aluminum plate. The edge of a second glass slide is then used to draw out the film by dragging the colloidal suspension across the surface. The main panel also shows the formation of primary cracks in region B. After the boundary between regions B and C has passed, the formation of less well ordered cracks is observed.

A critical quantity is the magnitude of the stresses that develop in the films during drying. Petersen et al.[11] and others[7,12,13] have measured the stresses during drying by coating a thin cantilever with a colloidal suspension. As the film dries, the cantilever deflects in response to the stress in the film. However, such measurements are complicated by the fact that the deflection must be decoupled from the changing weight of the film during evaporation of the suspending solvent. As a result, other spatially resolved techniques have subsequently been developed to measure the local stress in drying films.[14−16] Man et al.[17] were also able to measure the stress required to produce a crack that spanned the entire width of the colloidal film, by carefully controlling the vapor pressure of water in a drying chamber. These authors found that the measured stresses are independent of particle size. The different particle size dependencies reported in the above experiments suggest that the drying geometry and the drying dynamics may also influence the cracking process.

The role of substrate constraint in the cracking process has also been recognized.[17,18] Drying films on a liquid surface results in the substrate constraint being removed. Chiu et al.[9] dried films of 400 nm alumina particles on a liquid mercury surface and observed no cracking, highlighting constraint as an important factor. In this paper we provide important new evidence for the role of the substrate in both causing a drying film to crack and also controlling the crack spacing.

■ EXPERIMENTAL SECTION

Crack Formation Studies. Colloidal suspensions of polystyrene (PS) latices (10% solids content, Varian) were diluted to different concentrations using distilled, deionized water. The size distribution of

each of the latex particle suspensions used was measured using a ViscoTek dynamic light scattering apparatus, and the particle diameters were determined to be 47 ± 10 nm, 100 ± 16 nm, and 274 ± 44 nm, respectively.

Clean glass microscope slides (76 mm × 26 mm) were placed face-down on a clean lens tissue, and a fine marker pen was used to draw a labeled grid comprising ~15 mm × 10 mm rectangles on the reverse side of the slide. The glass slides were then placed face-up on a horizontal surface with one edge supported by a ~ 1 mm thick aluminum plate (see inset in Figure 1).

Thin colloidal films were cast onto the inclined glass substrates by placing droplets of the colloidal suspension along the bottom edge of the glass slides. The edge of a second cleaned glass slide was then used to draw the colloidal suspension along the glass substrate (see Figure 1). This resulted in a planar contact line at the suspension/substrate/air interface. The colloidal suspensions were then allowed to dry under ambient conditions (25 °C and relative humidity ~40%). The small angle of inclination of the substrate caused the colloidal suspensions to dry in one dimension with a planar drying front propagating down the glass slide (see Figure 1). The drying films were observed to display three distinct regions during drying. Region A consisted of a dilute suspension of the colloidal particles (see Figure 1). This region was followed by a *wet* region (region B) where the particles had been deposited at the contact line between the dilute suspension and the colloidal film. In this region the particles are close packed but the void space between the particles is occupied by water (as confirmed by IR microscopy measurements). The width of region B was observed to remain approximately constant during drying and was found to propagate behind the main planar front of the drying colloidal suspension. Region C corresponds to a completely dried film and could be clearly distinguished from region B because of the optical contrast between the two regions. As the films dried, cracks were observed to form in the 'wet' region of the films and were observed to propagate in a direction perpendicular to the drying front (and parallel to the drying direction). These cracks were found to have a well-defined spacing that depended upon the local colloid film thickness and were found to propagate at the same rate as the interface between the 'wet' and 'dry' regions. After the interface between these regions had passed a particular point on the drying films, secondary crack formation was observed. These secondary cracks were found to be less well ordered than the primary cracks mentioned above (see region C, Figure 1). These observations are consistent with other literature reports of drying colloidal films.[7,19]

Observation of the drying films using an Olympus IL70 inverted optical microscope showed that the primary cracks extended all the way down to the film/substrate interface and formed while the colloidal films were still attached to the substrate. This could be determined from the fact that there was similar optical contrast between the wet regions (region B) and the dilute colloidal suspension (region A) when viewed from below, indicating that the primary crack formation regions were still in intimate contact with the glass substrate. The formation of the secondary cracks (region C, Figure 1) was accompanied by a significant darkening in the regions of the inverted optical micrographs where these cracks were being formed. This was attributed to excess scattering at the film/substrate interface caused by the partial (and sometimes complete) debonding of the films from the glass substrate.

When the films had completely dried, the grid that had been drawn on the underside of the glass slides was used to identify regions on the films for collecting measurements. An Olympus BX51 microscope equipped with an Olympus DP70 digital camera operating in transmission mode was used to find a region where the grid lines intersected. The microscope was then set to reflection mode, and images of the crack patterns formed were collected at this location. The optical properties of the colloidal films were such that the grid lines could be observed in transmission mode, but not in reflection mode. Switching between the
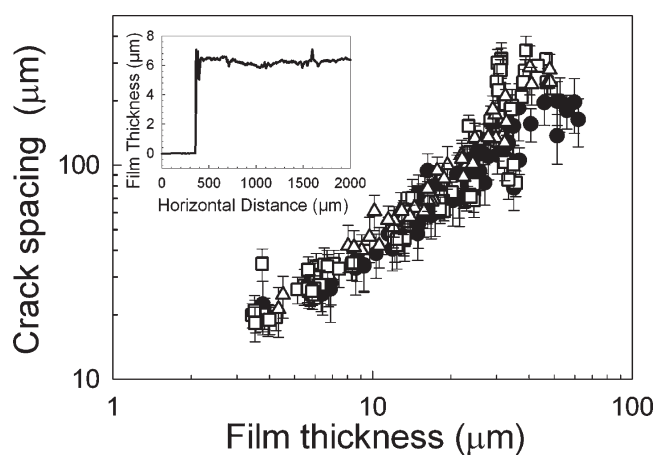
Figure 2. Average crack spacing as a function of the dry colloidal film thickness. Data are shown for colloidal films that were cast from suspensions of 47 nm ($\square$), 100 nm ($\triangle$), and 274 ($\bullet$) diameter particles, respectively. The inset shows variations in the local film thickness along a 2 mm scan of a 6 μm thick sample.

two modes provided a valuable way of reproducibly finding a particular region on the sample and collecting images which displayed only the crack patterns. All the images were flattened and analyzed using Image Pro Plus 4.0 image capture/analysis software (Media Cybernetics). The positions of all the cracks were then measured along a line on the image drawn perpendicular to the drying direction. The distance between successive cracks was calculated by determining where each crack intersected the line. The average crack spacing and its associated uncertainty were then determined at each grid position on the sample surface.

The colloidal films were then scored gently along the grid lines using a blunt scalpel blade. This was done to remove the colloidal films from the glass substrates so that the local thickness of the films at each of the grid positions could be determined. A Dektak[3] profilometer (Veeco Instruments) was then used to determine the local thickness at the intersection points of the grid lines on each sample. A typical trace showing a 2 mm line scan taken from a $\sim$ 6 μm thick dried colloid film of 47 nm particles is shown as an inset in Figure 2. The local thickness was found to vary slightly at different positions on the film due to the slight inclination of the samples during drying. However, it was found that the local thickness and crack spacing did not vary significantly in the regions used to obtain the optical micrographs. The main panel in Figure 2 shows a summary of the crack spacing as a function of the local film thickness for films cast onto glass surfaces from suspensions of 47 nm, 100 nm, and 274 nm diameter polystyrene particles.

Colloidal PS suspensions were also dried on liquid mercury surfaces and on a range of different elastomeric substrates to determine how the effects of the mechanical constraint imposed by the substrate influence the crack patterns that form.

Substrates with different Young's modulus values were prepared by cross-linking natural rubber (NR, polyisoprene, Sigma) with dicumyl peroxide (DCP).[20] In each case 45 g of NR was mixed with 5 g of a solution of DCP, dissolved at different concentrations in toluene. The solutions were mechanically mixed in a large glass beaker before being degassed in a vacuum oven at 50 °C for 4 h. The solution was then poured into rectangular (70 mm × 22 mm × 3 mm) PTFE molds. The molds were placed in an oven and heated for 2 h at 150 °C under a nitrogen atmosphere. At the same time, hemispherical PTFE molds of $\sim$5 mm in diameter containing the same elastomers were also prepared. After annealing, all the samples were allowed to cool and then carefully removed from the molds. The Young's modulus of the elastomers was

determined using an axisymmetric contact mechanics approach based upon the JKR method.[21] This method involved pressing the elastomer hemispheres into contact with a clean glass slide and measuring the contact area between the hemisphere and the glass slide as a function of the applied load. The rectangular elastomer films were attached to a glass substrate using double-sided adhesive tape and were inclined at an angle of 2° to the horizontal. Colloidal suspensions of 47 nm diameter particles were carefully spread over the surface of the elastomeric substrates using the edge of a clean glass slide. The films were then left to dry under ambient conditions.

Because of the lower wettability of the elastomeric substrates the colloid film thickness values (and hence the measured crack spacings) were found to be much larger than those of films that were dried on glass. The crack spacing on the elastomeric substrates was therefore measured using a high resolution camera. An image was collected of the whole glass slide and a steel rule was used as a scale bar. To measure the film thickness in the region containing the colloid film, the section of the elastomeric substrate containing the region of interest was gently cut and removed from the glass slide before being transferred on to a clean glass slide. The region was then photographed and the area of the sample section (A) measured using image analysis software. The film and elastomer substrate were then weighed before a lens tissue and toluene were used to carefully remove the polystyrene colloid film. The elastomer substrate was then left for 48 h to allow any solvent that had swollen the substrate to diffuse out. The substrates were then reweighed, and the difference in mass, M, was recorded. The thickness of the colloidal films was calculated using the formula $h = M/(\varphi \rho A)$ by assuming a particle volume fraction (φ) of 0.64[22] and a density (ρ) of polystyrene of 1050 kg m^{-3}.

As we are only interested in changes in behavior of colloidal particle films on elastomeric substrates, we note that the details of our analysis do not depend critically on the values of φ and ρ (or indeed the exact thickness of the colloidal films). The values used for φ and ρ may not represent the true values of these parameters in this study or the study on glass substrates mentioned above, but they are expected to be close and should result in the above formula giving a reasonable approximation to the thickness of the colloidal films.

During the drying of colloidal films on glass, it was found that some films had debonded from the substrate when they had dried out. It was therefore possible to carefully remove small sections of the colloidal films and image both the top (free) and bottom (previously in contact with the substrate) surface of the films using an atomic force microscope (MFP-3D, Asylum Research) operating in intermittent contact mode. The films dried on liquid mercury were also removed and imaged on both the top and bottom surfaces. The images were then Fourier transformed to reveal the structures formed by the particles in the films (see Figure 3).

Stress Measurements. The evolution of stresses in the drying colloidal films was measured using a variation on the cantilever deflection method reported by Petersen and co-workers and others.[7,11,12] In the experiments reported here, thin ($\sim$3 mm wide, $\sim$100 μm thick) glass cantilevers were prepared by cleaving rectangular glass coverslips into thin strips. The cantilevers were then clamped horizontally and leveled such that their free length (L) was set at 45 mm. The edge of the cantilever was then viewed from above using an optical microscope (see inset in top panel of Figure 4). A fine syringe needle was used to deposit and spread a small amount of a colloid suspension onto one of the vertical faces of the glass cantilever. The resulting films were then allowed to dry, and the deflection of the cantilever caused by the build up of stresses in the films was monitored using time lapse optical microscopy (see Figure 4). As the films dried, the cantilever was observed to deflect in the direction of the face supporting the drying colloidal film. This indicates that the films contract and exert a compressive stress on the cantilevers. The angular deflection of the
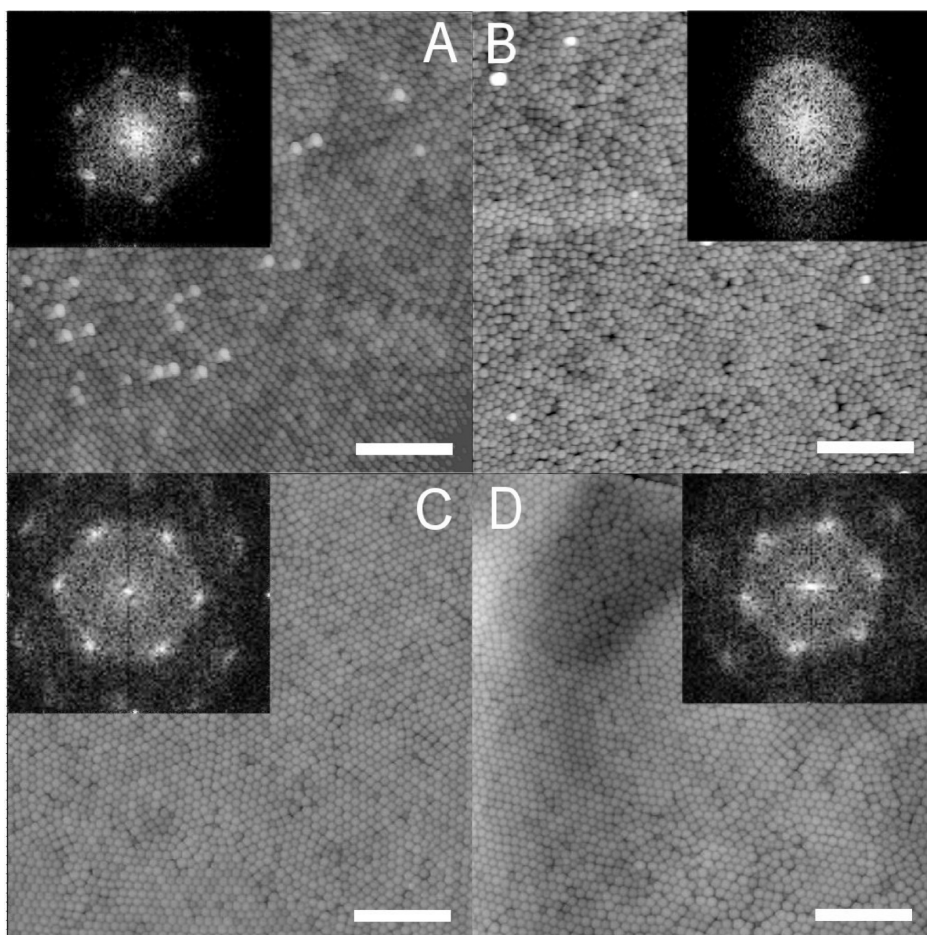
Figure 3. Atomic force microscopy of the arrangement of 100 nm particles in dried films. Debonding of the films from the substrate enabled both the top and bottom of the films to be imaged. Film dried on glass substrate: (A) top; (B) bottom. Film dried on liquid mercury substrate; (C) top; (D) bottom (scale bars: 1 μm). Insets show the 2D FFT of each of the images shown. A, C, and D show hexagonal close packing while B is randomly packed.

end of the cantilever was then determined from each series of optical micrographs obtained.

The stress in the films, σ_f, at each time point was calculated from the angular deflection, γ (measured in radians), using the equation.[11]

$$\sigma_f = \frac{E_c h_c^3}{6 h_f (h_f + h_c) L} \gamma \qquad (1)$$

where E_c and h_c are the Young's modulus and thickness of the glass cantilever, respectively, and h_f is the mean thickness of the colloid films.

In the above geometry, the weight of the drying film acts vertically and contributions due to the stresses in the films act horizontally. This therefore allows us to decouple effects due to changes in weight and the measured deflections that occur due to drying stresses that develop in the films.

After the colloid films on the cantilevers had dried completely, they were removed and scored, taking great care not to scratch the glass cantilever. This process was repeated at three separate positions on the film. A Dektak[3] profilometer was then used to measure the thickness of the colloid film at each position. The measured variations in the thickness obtained on the glass cantilevers were found to be much larger than those observed in the near horizontal drying geometry used in the crack formation studies. In particular, the films were observed to be thicker near the edges of the cantilever, and this was responsible for large uncertainties in the average film thickness and the stresses that were calculated using eq 1 (see Figure 4). The magnitude of the variations in film thickness across the surface of the glass cantilevers were found to depend on the particle

size used in the drying suspensions with smaller particles giving smaller variations. This was interpreted in terms of the differences in wettability that were observed for the different suspensions on the glass cantilevers.

■ RESULTS AND DISCUSSION

Figure 2 shows the dependence of the crack spacing (λ) on film thickness (H) for colloidal PS films cast on glass substrates. This figure clearly shows that the crack spacing increases as the thickness of the colloidal films increases in a way that is consistent with previous studies.[7] These data also clearly show that the crack spacing obtained is independent of particle size within the limits of experimental uncertainty for the three particles sizes studied. Previous studies of cracking in colloidal PS films by Lee and Routh[8] also show little or no particle size dependence of the crack spacing for samples that were cast using a similar drying geometry and over a similar range of thickness values to those discussed here. A recent model by Russel et al[6] also shows that the critical capillary pressure required to balance the interfacial energy needed for crack formation, and hence the crack spacing is expected to be independent of particle size.

There is a temptation to assume that the details of the drying geometry and deposition are not important. However, comparison with recent work by Cao et al[10] lends support to the idea that
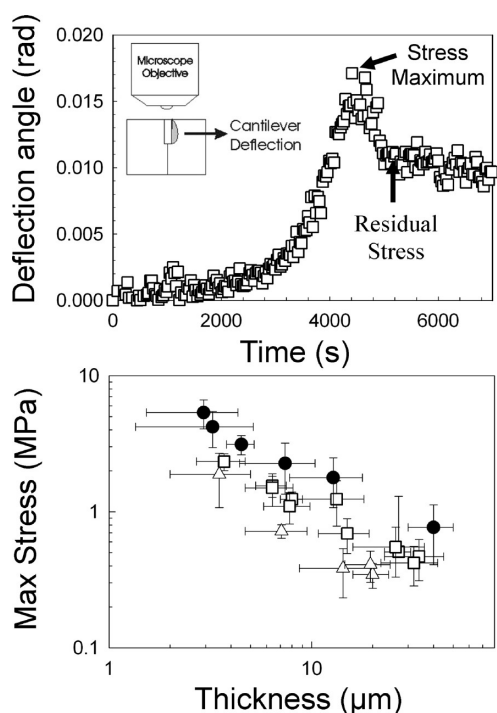
Figure 4. (Top panel) Angular deflection of a cantilever coated with a thin film of 47 nm colloidal polystyrene particles. Data are shown for a $15 \pm 4\,\mu m$ thick film (dry thickness) supported on a $102 \pm 1\,\mu m$ thick, 45 mm long glass cantilever. The bottom panel shows how the maximum stress varies as a function of the final (dry) film thickness. Data are shown for films cast from □ = 47 nm, △ = 100 nm, ● = 274 nm diameter particle suspensions.

these details can have profound effects on the observed behavior. These authors used a vertical drying geometry based upon a modified Langmuir−Blodgett approach which involved the very slow deposition of particles from a large reservoir, and they observed a clear particle size dependent crack spacing.

Attempts to measure the build up of stresses that drive crack formation during drying have largely focused on the cantilever deflection techniques first described by Petersen et al.[11] The top panel of Figure 4 shows the angular deflection of a glass cantilever coated with a thin film of colloidal suspension. The angular deflection is caused by the build up of stresses in the films[11] and increases with time (with a $t^{2.5}$ dependence) until a maximum is reached. The cantilever deflection then drops suddenly to a nonzero value, suggesting that some residual stress remains in the dried films. The sudden reduction of the angular deflection coincides with the appearance of fine cracks in the colloidal films similar to those described above. This indicates that the tensile stresses exerted on the drying films by the cantilever are partially relieved by the formation of cracks in the system. These observations are consistent with those reported by Tirumkudulu and Russel[7] and others.[18]

The particle size dependence of the stresses that are measured in these samples appears to be nontrivial (see Figure 4). Recent experiments and a theoretical model indicate that the maximum stress is independent of particle size.[7,23] Figure 4 shows that the calculated maximum stress values change but that they do not vary monotonically with particle size. The exact reasons for these variations in stress with particle size are not clear. However, it is worth noting that the stresses that developed in the films in this

study represent an average of the *effective stress* experienced by the entire film supported on the surface of the cantilever. Cantilever deflection measurements of this kind do not give information about the local stresses experienced by the drying films.[11] Interpretation of these stress measurements is also made difficult by a number of experimental factors relating to the way in which the films are formed.[6] First, a thicker rim of dried colloid is often observed to develop around the edge of the cantilever with a thinner film in the central region. Second, the entire film does not crack at the same point in time. These factors lead to uncertainties in the measurements of film thickness and the true maximum stress that is generated in the films. The nonmonotonic particle size dependence of the stresses may also be related to factors such as the differences in wettability and drying rates that were observed for the different particle sizes used in these experiments.

On the basis of these factors, it is unreasonable to place too great a confidence in the precision of the measured stresses (and the corresponding particle size dependencies) that are obtained using the cantilever deflection technique. However, these measurements still provide useful semiquantitative information about the thickness dependence of the stresses in the films. The monotonic decrease in stress with increasing film thickness for all particle sizes is particularly striking and is consistent with recent results obtained by Man et al. using an alternative approach.[6] One possible interpretation of the fact that the measured stress decreases with increasing film thickness involves the relative effect of interfacial confinement/constraint on the drying films. As the films are made thinner, the surface-to-volume ratio in the samples becomes higher and the influence of any surface/interfacial effects should become more prominent. For example, if we suppose that the stresses in the film are generated by a thin interfacial layer of thickness, h_o (which is likely to be approximately a few particle radii) in which the stress is σ_o, then if we average the forces over the entire film thickness, H, we obtain the following relationship for the thickness dependence of the average stress, σ, in the films.

$$\sigma = \sigma_o \frac{h_o}{H} \qquad (2)$$

This functional form is qualitatively very similar to that observed in the stress measurements shown in Figure 4 and also to the results of studies by other authors.[6] The question remains, however, as to whether the thickness dependence of the stresses are due to interfacial confinement effects in the drying films.

One way to determine if interfacial constraints are important in generating the stresses that drive crack formation in thin colloidal films is to manipulate the mechanical properties of the interfaces in such a way that any stresses that they might exert on the drying films can be varied. The simplest way to do this is to completely remove the substrate constraint by drying the colloidal film on a liquid substrate. This approach has been attempted previously by Chiu and co-workers who cast films on to mercury and managed to suppress crack formation in α-alumina films.[9] As reported above, we also observe no cracking of colloidal PS films on mercury surfaces. These simple yet powerful observations point very strongly to the fact that the substrate interface plays an important role in driving the cracking process in thin colloidal films and are in agreement with the theoretical model of Russel et al[6] which highlights the importance of in-plane constraints/tensile stresses in promoting crack formation.

Evidence for the existence of an interfacial strain in colloidal films drying on a rigid substrate can be obtained from AFM images of the top and bottom surfaces of the films formed on glass and mercury surfaces (i.e., the two extremes of the mechanical properties of the interface studied here). As discussed above, when drying out films of particles, some films were occasionally found to debond from the glass surfaces. This process occurred after the film was 'dry'. We were therefore able to carefully image both the top and bottom surfaces of the film with an atomic force microscope (AFM). Figure 3A and 3B shows the top and bottom surface of a 100 nm colloidal film that was cast on (and subsequently debonded from) a rigid glass substrate. Both the images and the 2D fast Fourier transforms of the images show clearly that there is a difference in packing between the free and substrate interfaces. The free surface exhibits hexagonal close packing (HCP), and the particles at the substrate interface exhibit random packing (as observed from the amorphous ring in the 2D FFT). Because HCP produces the maximum volume fraction of particles, it is unsurprising that particles rearrange to this configuration at the free surface under the large capillary stresses and slow time scales involved in the drying process. In contrast the bottom of the film exhibits no clear ordering as confirmed by the structureless FFT. Random close packing leads to a much less efficient packing at the substrate interface, and hence a mismatch strain exists between the top and bottom of the film.

AFM measurements of a film containing 100 nm particles, which was formed on a liquid mercury surface (Figure 3C,D), show that a similar ordering of particles is observed at the top (free) and bottom surfaces of the film. The distance between particles is therefore expected to be the same, and hence the mismatch strain between the top and bottom surfaces in these films is likely to be minimal. These observations suggest that in the samples studied here, thin colloidal films are formed via an initial random deposition/adsorption and sticking of particles at the substrate interface. As the films dry, the particles at the surface of the film will be pulled together under the action of capillary forces. This results in a HCP structure at the upper surface of the film, and if no constraint is provided by the substrate (as in the case of a liquid substrate), the stresses in the film also pull the particles at the bottom together until they adopt a HCP packing arrangement. Since there is no resistance from the substrate, the mismatch strain and hence any stored energy created by the capillary stresses would be negligible; there is thus insufficient energy to create crack interfaces. In the case of a rigid substrate, the interactions between the particles and the substrate would restrict the motion of adhered particles at the substrate interface and give rise to a difference in packing between the bottom and top surfaces of the film. As the film contracts under the influence of capillary forces at its surface, it will exert a compressive force on the substrate. The substrate then exerts an equal and opposite tensile force on the film. In the near substrate region, the influence of the substrate constraint is manifested as a difference in the interparticle spacings (or a mismatch strain) between the top and bottom surfaces of the film. If sufficient strain energy is stored in the film this would then result in the creation of crack surfaces.

In reality, the assumption that particles remain firmly adhered to the substrate may not be valid, as particles may still slip at this interface. Slippage at the substrate interface would enable the films to dissipate some of the strain energy generated in the films during drying. However, the interparticle spacings obtained from the AFM images shown in Figure 3 will still provide a good approximation to the final mismatch strain near the substrate, as these images were obtained from dried films after any slippage could have occurred. It is also worth noting that although we have imaged the top and bottom surfaces of the films in each case, a strain gradient does not necessarily have to exist throughout the entire film. It is much more likely that the random packing structure observed near the solid substrates will relax over distances that are comparable to a few particle diameters in order to relax any mechanical frustration in the films in a way that is comparable to the formation of strained layers in epitaxially deposited crystals.[24,25]

The rigid glass substrate and liquid mercury substrates represent the limiting cases (high and low, respectively) of the substrate mechanical properties. However, it is also possible to systematically vary the mechanical properties of the substrate by using elastomers with different cross-linking densities. As discussed above, capillary forces will cause the top surface of the film to form a HCP structure on these substrates, and this will in turn lead to forces on the layer of particles in contact with the elastomeric substrate. If the substrate is rigid, all the strain must be accommodated by the colloidal film, but if the substrate is sufficiently soft, some of the strain will be transferred to the elastomer. The strain energy density in the colloidal film will therefore decrease as the substrate modulus decreases and the amount of energy available to create new crack interfaces should be reduced, giving rise to a reduction in the crack density or an increase in the crack spacing. If this model is correct, then below a critical value of the substrate modulus the strain energy stored in the films would be expected to be unable to create new crack surfaces and the crack spacing should tend to infinity. Figure 5a shows measurements of the crack spacing as a function of film thickness for samples dried on elastomeric substrates with different modulus values. This plot clearly shows that the crack spacing increases with decreasing substrate modulus.

In order for a significant proportion of the strain energy to be stored in the elastomer, the film and substrate must have comparable values. Varying the Young's modulus of the substrate in this way should therefore enable us to obtain some measure of the mechanical properties of the colloidal films near the substrate interface. The mechanical properties of this system can be interpreted using a simple model which involves an infinitely thick compliant substrate, a layer of particles in contact and constrained by the substrate, and the rest of the colloidal film of thickness H (see inset in Figure 5b). We note that modeling the colloidal film as a continuum in this way results in some oversimplifications, such as ignoring the changing number of interparticle contacts. The modulus in reality probably changes at different stages during the drying process. The modulus used in the model presented below describes the situation where the particles are close packed and the interstitial spaces are filled with water.

The stresses that are generated in both the film and substrate are assumed to decay over small characteristic distances of $\sim h_o$ and $\sim l$ within the film and substrate, respectively, where h_o is on the order of one particle diameter and l scales with the characteristic spacing between cross-links in the elastomer substrate. The theory of rubber elasticity predicts that $l = (1/\alpha)(3kT/E_s)^{1/3}$,[26] where k is Boltzmann's constant, T is the temperature (Kelvin), and E_s is the Young's modulus of the substrate. The coefficient, α, is a constant which takes into account the fact that l is an approximation for the distance over which the stresses decay in the substrate. The true decay length in the elastomer substrate
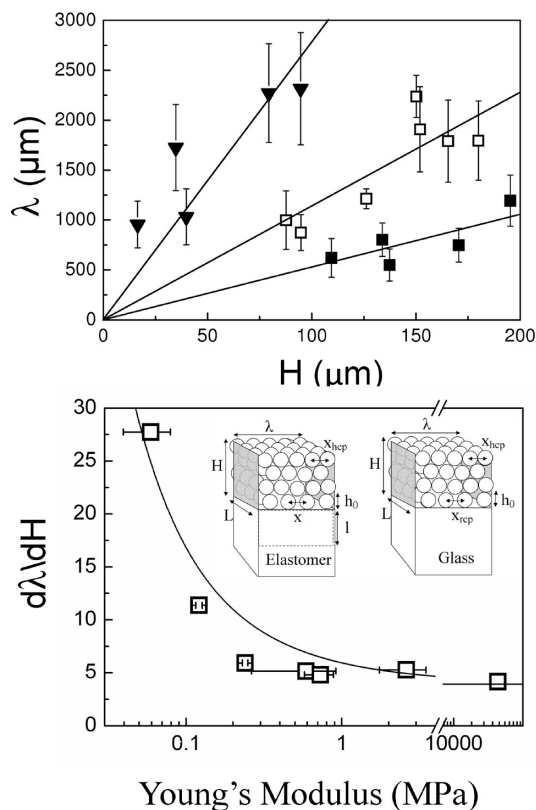
Figure 5. Influence of substrate modulus on crack spacing. (Top) The dependence of the crack spacing on film thickness for 47 nm PS particles. Data are shown for samples dried on 0.06 MPa (▼), 0.12 MPa (□), and 2.88 MPa (■) modulus elastomer substrates. (Bottom) Slope of the crack spacing vs film thickness curves ($d\lambda/dH$) for films of 47 nm colloidal particles dried on elastomeric substrates with different Young's moduli. The data points at 43 GPa are the $d\lambda/dH$ values for films that were cast on hard glass substrates. The solid line represents a fit to the form of $d\lambda/dH$ derived from eq 11. The parameters obtained from the fits were $E_{film} = 57.5 \pm 15.8$ MPa and $\alpha = (1.9 \pm 0.4) \times 10^{-4}$ MPa (see text). The inset in this panel shows diagrams of the proposed cracking geometry on hard (glass) and elastomeric substrates.

may be many times the typical separation between cross-links (e.g., $l \sim 1.8$ nm at $E_s \sim 1$ MPa), so α may be significantly smaller than unity. However, the scaling between l and the elastomer modulus obtained from the theory of rubbers is expected to be correct.

Assuming that the stresses in the film and substrate are distributed uniformly throughout layers with thickness values of h_o and l, respectively, the condition of force balance in the system gives an expression which relates the strains in the film and substrate (ε_f and ε_s, respectively) to the corresponding Young's modulus values E_f and E_s:

$$\varepsilon_s \approx -\frac{E_f h_o}{E_s l}\varepsilon_f \qquad (3)$$

A second relationship between the strains in the substrate and film can also be derived by considering the interparticle distances in the colloidal film and near the substrate interface (see inset in Figure 5). If the interparticle separation of particles at the interface is x and the interparticle spacing in the bulk of the film is x_{hcp} (where the particles are hexagonally close packed), the

tensile strain in the film becomes

$$\varepsilon_f = \frac{x - x_{hcp}}{x_{hcp}} = \frac{x}{x_{hcp}} - 1 \qquad (4)$$

On a hard substrate (such as glass), the deformations (and hence strains) in the substrate will be vanishingly small. At this point, the difference in particle spacings between the top and bottom surfaces of the films will be a maximum because the substrate experiences very little deformation. The tensile strain in the film will therefore be close to its maximum value. As the particles near the substrate interface randomly packed with an interparticle separation, x_{rcp}, the maximum tensile mismatch strain in the film ε_o, can be written as

$$\varepsilon_o = \frac{x_{rcp} - x_{hcp}}{x_{hcp}} = \frac{x_{rcp}}{x_{hcp}} - 1 \qquad (5)$$

As the substrate modulus is decreased, it becomes possible for some of this strain to be released by deformation of the substrate.

The strain in the substrate is obtained by assuming that particles adsorbed on the surface remain adsorbed and that they move with the substrate. Defining the displacements in the substrate relative to the zero substrate strain (random packing) condition above (see inset in Figure 5) gives a general expression for the substrate strain:

$$\varepsilon_s = \frac{x - x_{rcp}}{x_{rcp}} = \frac{x}{x_{rcp}} - 1 \qquad (6)$$

Note that in eq 6, the substrate strain is defined in the same sense as the film strain (i.e., as a tensile strain) but that $x < x_{rcp}$ so will have a negative sign, making it compressive. Eliminating x from eq 4 and eq 6 and using eq 5 to write the ratio $x_{rcp}/x_{hcp} = 1 + \varepsilon_o$ gives:

$$(1 + \varepsilon_f) = (1 + \varepsilon_o)(1 + \varepsilon_s) \qquad (7)$$

Expanding this expression and neglecting the small term $\varepsilon_s\varepsilon_o$ then gives

$$\varepsilon_f \approx \varepsilon_s + \varepsilon_o \qquad (8)$$

Combining this result with eq 3 and eliminating ε_s gives an expression for the strain in the film as,

$$\varepsilon_f = \frac{\varepsilon_o}{\left(1 + \dfrac{E_f h_o}{E_s l}\right)} \qquad (9)$$

The crack spacing in the films, λ, can then be derived using the Griffith criterion by equating the strain energy stored in a slab of volume λHL (see inset in Figure 5) with the energy required to create the crack interfaces. Assuming that the stresses are generated in a layer of thickness h_o within the films and that the cracks extend throughout the entire thickness, H, gives:

$$\frac{1}{2}E_f\varepsilon_f^2 h_o L\lambda = 2\gamma HL \qquad (10)$$

where γ is the surface tension of the colloidal suspension/film. Combining this eq 10 with eq 9 and inserting $l = (1/\alpha)(3kT/E_s)^{1/3}$

gives an expression for the crack spacing of the form

$$\lambda = \frac{4\gamma H}{E_f h_o \varepsilon_o^2}\left(1 + \frac{E_f h_o}{E_s l}\right)^2$$

$$= \frac{4\gamma H}{E_f h_o \varepsilon_o^2}\left(1 + \alpha\frac{E_f h_o}{(3E_s^2 kT)^{1/3}}\right)^2 \quad (11)$$

This equation predicts a linear dependence of the crack spacing upon the colloidal film thickness H which is in agreement with the results shown in Figures 2 and 5. It also predicts how $d\lambda/dH$ should vary with the substrate modulus E_s. At a first glance, this equation also seems to predict a particle size dependence of $d\lambda/dH$. However, it is worth noting that the Young's modulus of the film would also be expected to depend upon particle size. Previous studies by Cao and co-workers suggest that the film modulus should vary inversely proportional with particle diameter.[10] Such a particle size dependence of the Young's modulus of the film would give rise to a particle size independence of the cracking wavelength. However, in the absence of detailed experimental studies of the effects of particle size on the mechanical properties of the films it is difficult to draw any conclusions. At this point, we stress that this model represents a simple description of the physics which underlies the cracking process and that care should be taken to avoid making inferences about the particle size dependence of the cracking length scales in the absence of detailed experimental studies.

The value of ε_o can be determined from measurements of the difference in interparticle spacing obtained from FFTs of the randomly and hexagonally close packed particle structures observed in AFM images similar to those shown in Figure 3. This procedure gives a value of $\varepsilon_o = 0.16 \pm 0.01$ which is in good agreement with the theoretical predictions of the strain determined from the packing fractions of hexagonally and randomly packed particles. This number is also in agreement with a more simple method which involves calculating the difference in particle spacing by counting the number of particles per unit area in AFM images collected from the top and bottom of the film. Values of $\gamma = 72 \times 10^{-3}$ mJ m^{-2} and $h_o = 47$ nm were used for the surface tension of the colloidal suspension/film and the particle diameter, respectively, and the temperature was assumed to be 300 K.

The films dried on a glass substrate were used to obtain an approximation of the $d\lambda/dH$ value at infinite substrate modulus, giving $d\lambda/dH = 4.16$. Inserting the above values into eq 11 and letting $E_s \rightarrow \infty$ gives a value for the Young's modulus of the film of $E_f = 57.5 \pm 15.8$ MPa. This Young's modulus represents the tensile modulus of the film as defined in eq 3. We note that this is significantly smaller than the tensile modulus of Polystyrene ($\sim$3 GPa) which we would expect to be similar to the maximum value of the modulus that could be measured for particles in contact under compression. This is to be expected as the wet colloidal film is not an elastic continuum and actually comprises discrete charged stabilized particles which interact via DLVO forces. Cao et al.[10] suggest a value for the shear modulus based on mechanical measurements of samples containing polymer particles of $G = 34\gamma/R$ (where R is the radius of the particles) which for particles of 47 nm diameter gives a value of $\sim$100 MPa. The level of agreement between the modulus obtained and the predictions of the shear modulus is encouraging. Another estimate of the Young's modulus can be obtained by dividing the maximum capillary stress[17] $\sigma_{max} \sim 5.3\gamma/R$ by the measured

strain ε_0 obtained from the AFM studies presented here to give a value of $\sim$16 MPa. Given the simplifications made in formulating the model, it is encouraging that our value is of the same order of magnitude as these independently derived estimates of the modulus. Finally, it is possible to combine estimates of the measured mismatch strain with the value obtained for the Young's modulus to give a measure of the stresses that are generated within the drying colloidal film of $\sigma_f \sim E_f\varepsilon_o = 9.2 \pm 2.5$ MPa. This value is consistent with independent measurements of the magnitude of the stresses obtained from films dried on hard glass substrates shown in Figure 4.

Figure 5 shows a fit of $d\lambda/dH$ (obtained from eq 11) to the experimental data. The only adjustable parameter in the fit was α and the value obtained was $\alpha = (1.9 \pm 0.4) \times 10^{-4}$. This value is consistent with the fact that the estimates of both h_o and l should be used as approximations for the distances over which stresses decay away from the interface. The low value of α suggests that the strain in the substrate decays over many times the characteristic distance between cross-links in the rubber substrates (see discussion relating eq 3). However, the fact that the functional form of eq 11 can be used to fit the data in Figure 5 gives us some confidence that the scaling relation $l \propto E^{-1/3}$ is correct, at least to a first approximation.

A potential problem with this simple model is that it assumes that all the energy stored in the films is used to create the crack surfaces. However, the cantilever deflection measurements shown in Figure 4 suggest that some residual strain energy is stored in the films after cracking. This suggests that not all of the strain energy stored in the film is used to form the cracks. Another potentially important point relating to the delamination of the films on glass substrates is also worthy of discussion. The fact that the above model assumes that the particles are adsorbed at the substrate interface at first may appear to be inconsistent with the fact that the films were occasionally observed to delaminate. However, it is worth stressing that the films did not delaminate until they were completely dry. In the wet films the interactions between the particles and the substrate are likely to be different to those in the dried film. Moreover, the fact that secondary crack formation occurs in the films after the formation of the regular spaced cracks suggests that stresses continue to develop in the drying films. When the strain energy per unit area is larger than the work of adhesion (W) i.e. when $(1/2)E\varepsilon^2 h_o > W$, the film will debond from the substrate. As both the strain in the film ε and the work of adhesion are different in the wet and dry cases, it is not entirely unlikely that the particles would remain adhered in the wet films, but that the films would debond from the substrate when dried. Despite the fact that the model is oversimplified, the level of agreement between our simple analysis and the data obtained in Figures 2, 4, and 5 is encouraging. Our results suggest that this approach captures the key physics of the influence of substrate constraint mechanisms on cracking in thin colloidal films and can be used to obtain estimates of the Young's modulus of colloidal films E_{film} that are consistent with measured stress and strain values. Future studies will aim to try to overcome difficulties associated with differences in the wetting behavior of colloidal suspensions and will aim to determine the effects of changing the particle size on the measured *tensile* modulus of these samples.

■ CONCLUSIONS

This manuscript describes an experimental study of crack formation and stress development in thin colloidal films of

polystyrene particles. Cantilever deflection studies showed that the average stress in the films decreases with film thickness. These results were interpreted in terms of an increasing surface to volume ratio in thinner colloidal films and the effects of the mechanical constraints imposed by the substrate during drying of the films. Films that were cast onto liquid substrates where the mechanical constraint had been removed were shown to display no cracking. Similarly, the cracking behavior was modified by casting films on compliant elastomer substrates where the Young's modulus of the substrate was comparable to that of the drying colloidal film. Under conditions where the modulus of the substrate was smaller than the characteristic capillary stress, it was found that the crack density in the film was reduced (increased crack spacing). This modification in cracking behavior was interpreted using a simple model that considers the strains which develop within the drying film and substrate. This information was combined with the assumption that the strain energy stored in the drying films is balanced against the energy required to create the crack surfaces, to derive an expression for the dependence of the crack spacing on the substrate modulus and on the film thickness. These combined experiments and calculations provide convincing evidence that the constraint imposed by the substrate is an important factor in the drying induced crack formation of thin colloidal PS films.

■ AUTHOR INFORMATION

Corresponding Author

*E-mail: james.sharp@nottingham.ac.uk.

■ REFERENCES

(1) Dufresne, E. R.; Stark, D. J.; Greenblatt, N. A.; Cheng, J. X.; Hutchinson, J. W.; Mahadevan, L.; Weitz, D. A. *Langmuir* **2006**, *22*, 7144–7147.

(2) Singh, K. B.; Tirumkudulu, M. S. *Phys. Rev. Lett.* **2007**, *98*, 218302.

(3) Griffith, A. A. *Philos. Trans. R. Soc. London* **1921**, *221*, 163–198.

(4) Komatsu, T. S.; Sasa, S. *Jpn. J. Appl. Phys.* **1997**, *36*, 391–395.

(5) Alain, C.; Limat, L. *Phys. Rev. Lett.* **1995**, *74*, 2981–2984.

(6) Russel, W. B.; Wu, N.; Man, W. *Langmuir* **2008**, *24*, 1721–1730.

(7) Tirumkudulu, M. S.; Russel, W. B. *Langmuir* **2005**, *21*, 4938–4948.

(8) Lee, W. P.; Routh, A. F. *Langmuir* **2004**, *20*, 9885–9888.

(9) Chiu, R. C.; Garino, T.; Cima, M. J. *J. Am. Ceram. Soc.* **1993**, *76*, 2257–2264.

(10) Cao, H.; Lan, D.; Wang, Y.; Volinsky, A. A.; Duan, L.; Jiang, H. *Phys. Rev. E* **2010**, *82*, 031602.

(11) Petersen, C.; Heldmann, C.; Johannsmann, D. *Langmuir* **1999**, *15*, 7745–7751.

(12) Francis, L. F.; McCormick, A. V.; Vaessen, D. M.; Payne, J. A. *J. Mater. Sci.* **2002**, *37*, 4717–4731.

(13) Chiu, R. C.; Cima, M. J. *J. Am. Ceram. Soc.* **1993**, *76*, 2269–2277.

(14) von der Ehe, K.; Johannsmann, D. *Rev. Sci. Instrum.* **2007**, *78*, 113904.

(15) Konig, A. M.; Bourgeat-Lami, E.; Mellon, V.; von der Ehe, K.; Routh, A. F.; Johannsmann, D. *Langmuir* **2010**, *26*, 3815–3820.

(16) Xu, Y.; Engl, W. C.; Jerison, E. R.; Wallenstein, K. J.; Hyland, C.; Wilen, L. A.; Dufresne, E. R. *Proc. Natl. Acad. Sci. U.S.A.* **2010**, *107*, 14964–14967.

(17) Man, W.; Russel, W. B. *Phys. Rev. Lett.* **2008**, *100*, 198302.

(18) Holmes, D. M.; Vasant Kumar, R.; Clegg, W. J. *J. Am. Ceram. Soc.* **2006**, *89*, 1908–1913.

(19) Goehring, L.; Clegg, W. J.; Routh, A. F. *Langmuir* **2010**, *26*, 9269–9275.

(20) McKenna, G. B.; Flynn, K. M.; Chen, Y. *Macromolecules* **1989**, *22*, 4507–4512.

(21) Ahn, D.; Shull, K. R. *Macromolecules* **1996**, *29*, 4381–4390.

(22) Bernal, J. D.; Mason, J. *Nature* **1960**, *188*, 910–911.

(23) Yow, H. N.; Goikoetxea; Goehring, L.; Routh, A. F. *J. Colloid Interface Sci.* **2010**, *352*, 542–548.

(24) Budiman, R. A.; Ruda, H. E. *J. Appl. Phys.* **2000**, *88* (8), 4586.

(25) Tsui, Y. C.; Clyne, T. W. *Thin Solid Films* **1997**, *306*, 23–33.

(26) Jones, R.A.L. *Soft Condensed Matter*; Oxford University Press: Oxford, 2002.